On the identification of the angular position of gears for the diagnostics of planetary gearboxes

G. D'Elia[a,], E. Mucchi[a], M. Cocconcelli[b]

[a] *Engineering Department in Ferrara - Universitá degli Studi di Ferrara Via Saragat, 1 - 44122 Ferrara, Italy*

[b] *Department of Science and Engineering Methods - University of Modena and Reggio Emilia Via G. Amendola, 2 - Pad. Morselli - 42123 Reggio Emilia, Italy*

Abstract

Generally, in planetary gearbox diagnostics, vibration transducers are placed on the gearbox case near the ring gear. The relative angular position of the planet gears with respect to the transducer is a useful information for the evaluation of vibration signals related to planet/sun gears. This angular position is usually unknown, or it is known with a large tolerance causing serious difficulties in both gears and bearing diagnostics. In fact, noise and spurious component from healthy planets could overhang the informative content about incipient faults. The present work seeks to propose two alternative methods for the precise identification of the angular position of the planet gears with respect to the transducer. The first one is based on the study of how the power flows inside the Time Synchronous Average of the ring gear, whilst the second method is based on a modified statistical parameter such as the Crest Factor. The effectiveness of these methods is assessed on the basis of actual vibration signals acquired from a faulty planetary gearbox. The knowledge of the exact angular position of the planet gears allows the diagnostics of both gears and bearings, as proven by extensive experimental activities reported in the paper.

Keywords:
planetary gearbox, diagnostics, vibrations, time synchronous average

Email address: gianluca.delia@unife.it (G. D'Elia)

1. Introduction

Bearings and gears are probably the most common components in rotating machines. Since they are functional for the dynamics of the rotating parts, an incipient fault could lead to a sudden break of the machine. Thus, possible consequences are safety problems, irreparable damage of the machine, and high costs of non-production that normally exceed the cost of the machine. Consequently, the diagnostics of these components has always played a great interest in both academy and industry. The study of failure detection in bearings started over two decades ago, embracing a crowd of signal processing techniques which deals with several domains, from time to time-frequency. An emerging interest has been reported on modelling rotating machine signals as cyclostationary [1], which embodies a particular class in the realm of non-stationary stochastic processes [2]. From the pioneering work of McCormick and Nandi [3] the principles of cyclostationarity have become the state-of-art in bearing diagnostics [4]. Above all, Antoni in [5] discusses which cyclic spectral tool is the most suitable for the localised fault detection in ball bearings. In particular the operator that describes how the power flows within the signal was introduced by Antoni a few years ago [6]. Diagnostics becomes more complex when bearings and gears are coupled together as in gearboxes. Among them the class of planetary gearboxes is probably the most challenging. The difficulty of extracting the bearing characteristic fault frequencies of a planetary gear bearing stems from two factors. First, transducers may only be placed on the exterior of the gearbox, usually rather far from bearings. Second, the rotational axes of the planet gears are not fixed, i.e. they move with respect to the gearbox housing and thus to the transducers. As a result, the vibration signature of the planet gear bearings can be altered by the variable transfer path. In this scenario, standard signal processing techniques fail, and the characteristic bearing fault frequencies cannot be extracted from the vibration signals. For example envelope analysis, which is a widely used technique, could fail due to spurious components that overhang the fault signature. Indeed the working conditions of a specific gearbox could increase or reduce the fighting chance of the standard technique. Time synchronous averaging (TSA) has been shown to be a useful tool for extracting gear mesh vibrations from composite vibration signals since it enables the extraction of periodic signals from noise-polluted signals [7, 8, 9]. The resulting vibration signal corresponds to one complete revolution of the gear under consideration, and thus changes in the vibration waveform due to damage on individual teeth can be identified. The application of the TSA for the extraction of periodic waveforms in ordinary gearbox was proposed by Braun in the mid 70s [7]. However, such TSA techniques relate to gears with fixed vibration transfer paths from the source of the vibration to the transducer. In planetary gearboxes, the vibration transfer path is not fixed but it is subjected to variation due to the relative motion of the planet gears with respect to the transducer.

A technique for the evaluation of the TSA vibration signals associated with the sun and planet gears of a planetary gearbox was proposed by P.D. McFadden in the early 90s [10]. Such a work demonstrates that, for planetary gearboxes with certain geometric properties, the averaged vibration signals can be extracted from a vibration signal captured by a single fixed-frame transducer. Subsequent studies validated the McFadden's research and presented slight variations on the technique [11, 12]. Samuel and Pines [12] incorporates the use of multiple sensors in the evaluation of planet and sun gear TSAs. The use of multiple sensors overcome several limitations such as: i) capturing all the teeth of planet and sun gear in planetary gearboxes with non appropriate geometric properties, ii) reduce the time required for performing the planet and sun gear TSAs and iii) increasing the robustness of the extraction method in case of sensor failure. However, the fundamental methodology remains unchanged; moreover [12] does not focus the attention on the evaluation of the relative position between planet gears and transducer.

The TSA of the planet/sun gears can be obtained if and only if, the relative position of the planet gears with respect to a transducer placed on the ring gear is known a priori. In [13] McFadden suggested that the position of each of the planet gears with respect to the transducer, could be estimated directly from the TSA of the ring gear by identifying the locations of the maximum vibration amplitude. This identification could be more effective from the amplitude modulated signal of the ring gear. For small planetary gearbox, this approach could be not effective and the planet position cannot be identified leading to a poor evaluation of the planet gear TSA, as outlined in the following.

This paper focuses on fixed ring gear epicyclic gear train working on the hypothesis of steady speed. In particular two alternative methods are proposed for the precise identification of the position of each of the planet gears with respect to the transducer. Once the vibration signal related to each gearbox components is determined, diagnostics of gears is straightforward by means of anyone of the established method proposed in the literature. Moreover, also the diagnostics of the gearbox bearings is now possible, since Cyclic Power technique works on a vibration signal which is free from components other from the one under study. The aim of this paper is to propose a methodology for the diagnostics of a planetary gearbox as a whole, including both gears and bearings.

The paper is organised as follows. After a brief introduction and problem statement given in this Section, the TSA algorithm proposed by McFadden is outlined in the next. The two proposed methods for the evaluation of the planet gear positions are presented in Section 3. The effectiveness of the proposed diagnostics methods is discussed on the basis of real data in Section 4 for both gears and bearings. Section 5 addresses the concluding remarks.

2. Background on TSA in planetary gearbox

McFadden and Smith [14] have demonstrated that as a given planet gear approaches the transducer, the measured vibration level increases, while as the planet gear moves away from the transducer the measured vibration level decreases. Let introduce $h(t)$ the transfer function between the transducer and the planet gear, with a period of one carrier revolution T_c, Figure 1. Thus, planet signal $x(t)$ as seen by transducer j is given by $h_j(t)x(t)$.

In order to extract the planet/sun signal McFadden stated that [14] : *"when a given planet gear is near a transducer, the vibrations measured by the transducer are dominated by the meshing of that specific planet gear with the sun and ring gears."* Thus, during each passing of a given planet, a small data window can be collected. It can be assumed that over the width of such a window, the transfer function between the accelerometer and the region of tooth contact will remain constant. The planet gear teeth in mesh can be determined at each carrier revolution, and the window of data can be stored in a buffer according to the meshing tooth. This process is then repeated several times, in order to obtain a window of data for each tooth of the planet gear. The so arranged buffer includes the vibration signal for a complete revolution of the planet gear. Several buffers can then be averaged in order to obtain the TSA signal of the gear of interest, Figure 2.

Mathematically speaking, let define a windowing function centered at time $t = nT_c$, where n is an integer number. The time at which $h_j(t)$ reaches its maximum is defined by $v(t-nT_c)$, Figure 1 (c). The subsequent windowed vibration signal is given by expression $h_j(t)x(t)v(t-nT_c)$.

Let the window width be chosen as an integer number of tooth mesh period T_m, given by [13]:

$$T_v = N_v T_m \tag{1}$$

If N_v is chosen to be appropriately small, the amplitude of $h_j(t)$ can be assumed to be constant ($H_{j,0}$) over the entire window, and the vibration signal becomes:

$$h_j(t)x(t)v(t - nT_c) = H_{j,0}x(t)v(t - nT_c) \tag{2}$$

Once a window of vibration data has been obtained, it must be mapped into the appropriate location in a buffer for synthesizing the planet/sun gear vibration signal. To determine this location a sampling function $g(t) = g(t - nT_g)$ can be used, where T_g is the rotation period of the gear of interest (planet/sun). The convolution operator can be used, leading to $[H_{j,0}x(t)v(t - nT_c)] * g(t)$, in order to map the windows into the appropriate location. If the tooth number of the gear of interest is N_g, once N_g windows have been mapped, all of the teeth of the gear under consideration will be captured.

In order to extract the TSA vibration signal from the measured one, a large number (N_e) of synthesized signals (buffers) must be captured and averaged. The TSA of the gear of interest is given by:

$$x_g(t) = \frac{1}{N_e N_v} \sum_{n=0}^{N_e N_g - 1} [H_{j,0}x(t)v(t - nT_c)] * g(t) \tag{3}$$

Therefore, in order to compute the planet/sun gear TSA, the signal should be firstly angular resampled according to the period of rotation of the gear of interest (T_g). In order to do that, the carrier rotation frequency must to be known; the rotation period of the gear of interest could be obtained by multiplying the carrier rotation period by the Willis gear ratio between ring gear and the gear of interest.

The number of carrier rotations that occur before the gear of interest will return to its initial state relative to the ring gear is given by:

$$n_{Reset,g} = \frac{lcm(N_g, N_r)}{N_r} \tag{4}$$

where lcm stands for least common multiple and N_r is the number of ring gear teeth. Therefore, a given tooth of the gear of interest will be aligned (in case of planter gear, alignment implies meshing) with a given tooth of the ring gear for a given carrier rotation only once every $n_{Reset,g}$. For each carrier rotation, the sequence of aligned teeth can be found using:

$$P_{n,g} = mod(nN_r, N_g) + 1 \tag{5}$$

where *mod* is the modulus after division and n is the number of carrier rotations. The tooth aligned in the initial state, $P_{0,g}$, is defined as tooth 1. It can be seen that $P_{0,g} = P_{n_{Reset},g}$.

3. On the planet-transducer position

Function $h(t)$ is directly related to the mass, damping and stiffness properties of the gearbox. In some cases the combination of these properties leads function $h(t)$ to be particularly flat. Thus, no amplitude modulation effects can be visible in the ring gear TSA, also after the application of the amplitude demodulation techniques, e.g. the Hilbert Transform demodulation [15] or the McFadden's separation method as well [13]. The planet gear position relative to the transducer cannot be pointed out, leading to a poor evaluation of the planet gear TSA. Hereafter two methods are proposed in order to identify the angular position of the planet gears with respect to the transducer. The first one is based on the mean instantaneous power of the ring gear TSA, whilst the second one is based on a "modified" Crest Factor.

3.1. Method A: Power flow

The relative position of each of the planet gears with respect to the transducer could be estimated by studying how the power flows in the vibration signal. In particular, the planet position could be determined from the power flow of the ring gear TSA. As a matter of fact, each time a planet passes under the transducer, an increase of the power released within the signal occurs.

The operator that describes how the power flows within the signal was introduced by J. Antoni a few years ago [6]. Let $x(t)$ be a continuous time signal, the mean instantaneous power is defined as:

$$P_x(t) = \sum_{\alpha \in \mathcal{A}} P_x^{\alpha} e^{j2\pi\alpha t} \tag{6}$$

where P_x^{α} is the cyclic powers of the signal at cyclic frequencies α, defined as:

$$P_x^{\alpha} = \lim_{T\to\infty} \frac{1}{T} \int_T |x(t)|^2 e^{-j2\pi\alpha t} dt \tag{7}$$

Set $\mathcal{A}$ in equation (6) embraces all the cyclic frequencies inside $x(t)$.

In order to obtain the position of the planet gears with respect to the transducer, the cyclic power is filtered around the cyclic frequency corresponding to the number of gear teeth, with a bandwidth large enough to encompass a number of sidebands corresponding to the number of the planetary gearbox planets. In particular, the whole procedure could be summarised as follows:

- Evaluation of the ring gear TSA
- Evaluation of P_x^{α} relative to the ring gear TSA (i.e. estimation of the Fourier Transform of the squared absolute value of the ring gear TSA)
- Inclusion in set $\mathcal{A}$ of the cyclic order equal to the number of the ring gear teeth, as well as the left and right modulating sidebands corresponding to the number of planet gears (i.e. filter the P_x^{α} by taking into account only the cyclic order equal to the number of ring gear teeth as well as both the left and right sideband relative to the number of planet gears)
- Reconstruction of P_x based on set $\mathcal{A}$ (i.e. estimation of the inverse Fourier Transform of the filtered P_x^{α})
- Evaluation of the envelope of P_x
- Every maxima in P_x envelope will give the time instant corresponding to a constant phase value of successive planet with respect to the transducer location.

Once one planet gear phase is evaluated, the phases of the other planet gears can be obtained by taking into account the angle between two consecutive planet gears by kinematics relations, or by taking into account the other maxima.

3.2. Method B: Statistical Parameter

The position of a particular planet gear with respect to the transducer can also be determined by the analysis of a simple statistical parameter. A counterpart of the function P_x can be obtained by a tooth-wide evaluation of a "Moving Crest Factor"(MCF). The MCF is defined as:

$$MCF = \frac{x(\tau)_{peak-peak}}{RMS(x(\tau))} \tag{8}$$

where $x_{peak-peak}(\tau)$ is the peak to peak value and $RMS(x(\tau))$ indicates the RMS value. Time parameter τ is used to stress the moving windowed nature of the signal: $x(\tau) = w(t - \tau_w))x(t)$, where w is the windowing function and τ_w the delay used according to the following procedure. Generally speaking, the Crest Factor is a measure of how extreme the peaks are in a waveform compared to the mean value. The peak to peak value is used in equation (8) in order to increase the sensitivity of the genuine Crest Factor. The MCF evaluated by equation (8) is not a function of time, but a single numerical value. In order to obtain a function which could be related to the signal power flow, Eq. (8) is evaluated on a signal portion embracing a single ring gear tooth. Finally, the tooth-wide MCF is filtered around the order of the planet carrier rotation which corresponds to the planet gear number. De facto, the evaluation of MCF over a one tooth wide window, set its sample frequency equals to the number of ring gear teeth. Because the frequency range of interest is related to the number of planet gears, the sample frequency of MCF is always greater enough to perfectly reconstruct the waveform of interest. The maximum value of the so processed MCF gives the position of one planet gear with respect to the transducer. The whole procedure could be summarised as follows:

- Evaluation of the ring gear TSA
- Evaluation of the MCF for each ring tooth
- Filtering the tooth-wide MCF function around the order of the planet carrier rotation which corresponds to the planet gear number
- Every maxima in the filtered tooth-wide MCF function will give the time instant corresponding to a constant phase value of the successive planet with respect to the transducer location.

As previously stated, once one planet gear phase is evaluated, the phases of the other planet gears can be obtained by taking into account the angle between two consecutive planet gears, or by taking into account the other maxima. Moreover, phase distortion should be avoided during the filtering operation. In this work an ideal FIR filter is used, which does not affect the phase of the filtered signal.

Table 1: Induction motor data

	BN80C2	BN132MB4
Nominal power $[kW]$	1.5	9.2
Nominal torque $[Nm]$	5.1	61
Nominal speed $[rpm]$	2800	1440
Number of poles per phase winding	2	4

4. Experimental data analysis and discussion

This section aims at testing the effectiveness of the proposed methods for both the diagnostics of gears and bearings on the basis of experimental data. Tests were performed in a test-rig designed and built up at the Engineering Department of the University of Ferrara. The test-rig consists of a base, including two induction motors controlled by inverters and a planetary gear unit (Figure 3). In more detail, the driving induction motor (BN80C2) is controlled in a feedback speed loop; its speed is evaluated by an encoder with 360 pulses per revolution. The load induction motor (BN132MB4) is controlled in a feedback torque loop by measuring the current absorbed in the working condition, while the speed is evaluated by an encoder with 3600 pulses per revolution. Table 1 lists the data of the induction motors.

The tests were performed on a two-stage planetary gearbox. In particular, the gear unit (MP 105 IS 2) is a two-stage on which each stage contains a sun gear (27 teeth), three planets (39 teeth) and a ring gear (108 teeth) for a global speed reduction ratio of 25. Table 2 lists the data of each gearbox stage, while Table 3 lists the aligned tooth of the gear planet with a given tooth of the ring gear under the transducer, from 0 to 12 carrier rotations (Equation 5). De facto, after 13 carrier rotations the planet gear return to its initial state under the transducer (Equation 4). It is possible to see from Table 3, that the minimum width of the window function allowing for a complete reconstruction of the planet signal is 3 teeth. As stated in [13], in order to reduce the error component in the planet signals, the windowed signal extracted for each carrier rotation should overlap, therefore a window

Table 2: Gear data

	First stage	Second stage
Sun gear teeth	27	36
Planet gear teeth	39	39
Ring gear teeth	108	108
Number of planets	3	3
Speed reduction ratio	5	4

Table 3: Sequence of planet gear teeth under the transducer for each carrier revolution, Equation 5

carrier rotation n	0	1	2	3	4	5	6	7	8	9	10	11	12
tooth #	1	31	22	13	4	34	25	16	7	37	28	19	10

embracing 5 ring gear teeth is chosen for all the analysis carried out in this work. Figure 4 depicts such a window, which is a rectangular window with cosine tapered ends where the central part is 3 teeth width with an overlap factor of 2 teeth.

Localized faults in planet gear are taken into account in the first test, while a planet bearing fault is considered in the second test. Such two tests are presented and discussed in the following subsections.

4.1. Gear analysis

Two localised tooth faults were artificially introduced on one planet gear of the gearbox first stage. Figure 5 depicts the two faults, namely LFP1 and LFP2. The dimensions of the faults related to axial length of the tooth are 14% and 45% respectively for LFP1 and LFP2. In particular, LFP1 is a small tooth fault introduced on the tooth flank with an electric pen drive. The LFP2 fault, which is introduced via a drilling process, embraces approximately half of the tooth flank.

During tests, the vibration signals were acquired by means of a piezoelectric accelerometer (frequency range 1 to 12000Hz) mounted in radial direction on the gearbox case near the ring gear. A one pulse per revolution optical tachometer is mounted on the gearbox output shaft (planet carrier). Signals where acquired for an extent of 60s with a sample frequency of 204.8kHz. This high sample frequency guarantees to properly acquire the tachometer signal. Vibration signals were subsequently downsampled at 5.12kHz during post processing, in order to embrace the first five meshing components. Tests were performed at different conditions of driving speed and applied torque. The results presented in this work are relative to a nominal driving motor speed of 20Hz and nominal output shaft torque of 12Nm.

Figure 6 depicts the time signals captured from the accelerometer for both sound and faulty conditions. The vibration amplitude related to the two fault conditions is not increased compared to the sound one. In particular, the modulation effect due to the planet gear passage toward the accelerometer is not visible.

Diagnostics informations about the faulted planet gear can be obtained by extracting the signals of each planet gear from the global vibration signal captured by the accelerometer. In order to do that the TSA technique proposed by McFadden [10] can be used. The application of this technique relies on the knowledge of the position of the planet gears with respect to the accelerometer. This position can be determined from the ring gear TSA by identifying the locations of the maximum vibration amplitude. Figure 7 depicts the ring gear TSA for both sound and faulted conditions. The three ring gear TSAs are essentially the same, sure enough these represent the ring gear signal which does not change from the sound to the faulty gearbox conditions. The relative position of each of the planet gears with respect to the transducer is not visible. Because of the geometrical and material properties of the gearbox under test, the transfer function between the transducer and the planet gear (Figure 1 (b)) is flat for the most part. This is mainly due to the mass, damping and stiffness properties of the gearbox. In this case the position of the planet gears is not detectable with the amplitude demodulation techniques, leading to a poor evaluation of the planet gear TSAs. In particular, Figure 8 depicts the results of the amplitude demodulation [15], where a filter bandwidth of 18 orders around the first (Figure 8(a)), second (Figure 8(b)), third (Figure 8(c)) and fourth (Figure 8(d)) meshing component is used in order to extract the amplitude modulation from the sound ring gear TSA. As stated before, no interesting information about the position of the planet gears can be obtained with this analysis due to the flatness of the transfer function $h(t)$.

Figure 9 depicts the core of this work. In particular, Figure 9 shows the results of the application of the two proposed methods on the ring gear TSA for both the LFP1 and LFP2 fault conditions, respectively. The two methods, the first one based on the P_x and the second one based on the MCF, give very close results, i.e. the points related to the maxima and minima of the two functions are almost the same. Small differences of 1-2 teeth proved to not change the output results, and for that reason only the P_x-method results will be shown in the figures later on.

In particular, it is possible to see that for the case of the LFP1 fault (Figure 9 (b) and (c)) the first maximum is reached around ring gear tooth 8. This means that the starting position of one planet gear, which could be the planet gear 1 without loss of generality, is shifted of an angle covered by 8 ring gear teeth with respect to the transducer. By inspecting the other two maxima of the functions, or via geometric considerations, one can conclude that the other two planet gears are shifted by an amount of 44 and 80 ring gear teeth with respect to the transducer (Figure 9 (b) and (c)). Analogous considerations can be performed for the LFP2 fault. Specifically, the first maximum is reached around the same ring gear tooth 8, which means that one planet gear is shifted of an angle covered by 8 ring gear teeth with respect to the transducer (Figure 9 (e) and (f)). The other two planet gears are shifted of 44 and 80 ring gear teeth, respectively.

In order to asses the validity of the proposed methodology, the vibration signal of the planet gears are extracted with an increasing shift from 1 to 108 ring gear tooth. Therefore, 108 planet gear TSAs are obtained, the Peak Hold of these TSAs (i.e. the maximum amplitude value of each TSA) is taken into account and compared with the results of P_x and MCF in Figure 9. It is possible to see a good match between the maximum values in the P_x and MCF functions with respect the Peak Hold of the planet gear vibrations. In particular, for the LFP2 fault (Figure 9 (d)) it is possible to see an encreasing in the amplitude content on a range of 30 ring gear teeth under the transducer, while for the LFP1 fault a small portion of about 5 ring gear teeth is affected by a small amplitude increase. This position information can be used in order to extract the vibration signal of the planet gears with the TSA technique proposed by McFadden. Figure 10 depicts the result of this operation for the LFP1 fault case, where the starting position of the averaging process is obtained by shifting the vibration signal of an angle covered by 8 ring gear teeth (first maximum int the P_x function). The averaging process can extract the vibration signal related with each planet gear in a precise manner. As depicted in Figure 10 (a) a small variation of the vibration amplitude can be seen in the planet gear 1 TSA. This small amplitude variation is not suitable for a sure fault detection and further analyses are needed. In particular, Figure 11 compares the results of the extraction of the planet gear 1 TSA with three different signal shifts. In

Figure 11 (a) the signal is shifted of an angle covered by 8 ring gear teeth, which is the closest position between transducer and planet gear. In Figures 11 (b-c) the signal is shifted of an angle covered by 35 and 62 ring gear teeth, respectively.

The first shift (i.e 35 teeth) correspond to the midpoint between the closest and the farthest position of the planet gear 1 with respect to the transducer, whilst the last shift, which corresponds to a minimum of both P_x and MCF functions, is the farthest position of planet gear 1 with respect to the transducer. As one can see, no evidence of variation in the vibration amplitude can be detected in Figures 11 (b-c). This result highlights the importance of the knowledge of the relative position of the planet gear with respect to the transducer, in particular for function $h(t)$ particularly flat. Figure 12 plots the result of the TSA of the planet gears for the LFP2 fault case. These averages are performed by shifting the signal for an amount corresponding to the first maximum of the P_x and MCF functions (i.e. 8 ring gear teeth). It is possible to see a strong variation in the signal amplitude of the planet gear 1 TSA (Figure 12 (a)), which corresponds to the artificial fault LFP2 inserted in the planet gear during test, and in addition, other two small variations are visible around tooth # 24 and 26. These amplitude variations are probably related to tooth profile errors which were already existent in the planet gear before test, due to the manufacturing process.

As in the case of LFP1 fault, Figure 13 compares the results of the extraction of the planet gear 1 TSA with three different signal shifts. The first one deals with the first maximum of the P_x and MCF functions (i.e. 8 ring gear teeth), which is the closest position between transducer and planet gear; the second one refers to the midpoint between the closes and the farthest position between transducer and planet gear; the third one refers to a minimum in the two functions which is the farthest position of the planet gear 1 with respect to the transducer (i.e. 62 ring gear teeth). Comparing Figures 13 (a), (b) and (c), it is possible to see that when the planet gear is near the transducer, the engaging of the faulted tooth can be well highlighted, whereas it could be merely visible leading to a poor fault identification. This result indicates that the proposed methodologies are effective for the evaluation of the planet gear position with respect to the transducer, leading to the detection of the faulty planet gear. In particular, if the real position of the planet gear with respect to the transducer is not correctly determined, the signature of the faulty planet gear cannot be suitably extracted from the noisy vibration response.

Table 4: Planet bearing data

Needle number	17
Needle diameter [mm]	2
Mean bearing diameter [mm]	11
Pressure angle [deg]	0

4.2. Bearing analysis

Planet bearings are full-complement needle bearings without cage. This arrangement consists of a collection of rollers arranged loosely between the pin, which connects the gear to the carrier, and the bore of the gear. The pin and the gear bore act as inner and outer races, respectively (Figure 14 (a)). A localised fault was artificially introduced on the inner ring of a planet bearing (carrier pin) via a drilling process. The angular length of the fault is $28deg$, the depth is approximately $0.5mm$ and the axial length is the 65% of the inner ring width. Figure 14 shows a full-complement needle bearing of the MP105IS2 planetary gearbox as well as the localised fault under test. Bearing data are depicted in Table 4.

The test set-up is the same presented in Sec. 4.1. The only differences are the mounting position of the optical tachometer, which is placed on the gearbox input shaft (first stage sun gear), and the downsampling frequency of the vibration data that is set at 51.2kHz.The fault on the bearing has been tested at two different torque loads only (12 Nm and 0 Nm). The results shown hereafter are consequently related to the loaded case.

Figure 15 depicts the time signals captured from the accelerometer for both sound and faulty conditions. Once again the vibration amplitude related to the faulty condition is not increased compared to the sound one. In particular, the RMS and Kurtosis values evaluated on the time signals for both the two conditions are essentially the same, i.e. $\mathrm{RMS}_{\mathrm{Sound}} = 2.18\mathrm{g}$ and $\mathrm{Kurt}_{\mathrm{Sound}} = 4.7$, $\mathrm{RMS}_{\mathrm{Fault}} = 1.89\mathrm{g}$ and $\mathrm{Kurt}_{\mathrm{Fault}} = 5.8$. Only the kurtosis value shows a small increment, however this increment does not justify the presence of a bearing fault. Figure 15 could also be compared with Figure 6, in both cases the diagnostics of faults is almost impossible without a proper pre-processing of the data.

Figure 16 shows the corresponding spectra. It is possible to see that for both conditions the components dominating the spectra are related to the meshing frequencies of the two stages. In more detail, the first stage meshing frequency is 432Hz whilst the second stage meshing frequency is 86.4Hz. Sidebands arise around the two meshing frequencies for both sound and faulty conditions. It is a matter of fact that in planetary gearbox sidebands are not related to the presence of a fault but are due to the relative motion of the planets with respect to the accelerometer which is mounted on the ring gear. An increase of the amplitude of the sidebands around the first stage meshing frequency is visible in Figure 16 (b). In particular, these sidebands are related to the rotation frequency of the first stage carrier. This effect could be associated to an abnormal rotation of the first stage carrier resulting from an abnormal gear planet rotation due to the planet bearing fault. In his well known handbook on gear analysis, Taylor [16] states that when the amplitude of the sidebands on the low side of gear mesh frequency is higher than the upper sidebands, looseness is indicated. In Figure 16 (b) the lower sideband (428 Hz) is quite higher than the gear mesh frequency (432 Hz), pointing out a looseness condition in the planet gear with the faulted bearing. Moreover, no evidence of a resonance zone excited by the impulses produced by the fault is present in the frequency domain between 0 Hz and 25.6 kHz. These results cannot provide proper diagnostics information and additional analyses have to be carried out.

Figure 17 shows the Cyclic Spectra for both sound and faulty conditions. It is possible to see that there is a strong release of power at the rotation frequency of the first stage planet carrier (4Hz) and its harmonics. In particular, for the faulted condition (Figure 17 (b)), there is a strong modulation of the rotation frequency of the first stage planet carrier by the rotation frequency of the second stage planet carrier (0.8Hz). This effect could be related to the floating sun gear arrangement applied in this type of gearbox.

It is a matter of fact that in planetary gearbox the radial loads acting on the sun cancel out, and therefore fixed radial bearings are not necessary to support the sun gear itself. However, the localised fault in the planet bearing causes an incorrect engagement between the planet and the sun. This phenomenon could produce an irregular radial displacement of the sun gear during its rotation, which manifests itself as a modulation of the sun rotation frequency. Actually, these results can highlight the malfunctioning behaviour of the planetary gearbox. However, no diagnostics information such as the type and the position of the fault can be obtained, in particular, the cyclic frequency of the inner race fault (111.2725Hz) is not visible inside the signal Cyclic Spectrum (Figure 17 (b)).

Diagnostics information about the faulted planet bearing can be obtained by extracting, from the global vibration signal captured by the accelerometer, the signals of each planet gear. In particular the power flow method has been used in this paper in order to find the initial angular position of the planets with respect to the transducer. In order to do that the TSA technique proposed by McFadden [10] can be used. De facto, the TSA signal is only the deterministic counterpart of the raw signal, while the bearing fault information is included in the second order cyclostationary counterpart. Therefore, the bearing analysis is performed on the extracted planet signal before averaging. After that, by the evaluation of the Cyclic Power on the extracted signals it is possible to obtain information on how the power is released by that particular component, highlighting the presence of a fault in a particular planet bearing. The extracted planet signals are in the angular domain, thus the corresponding Cyclic Powers belongs to the the cyclic order domain. The link between cyclic orders and cyclic frequencies is the rotation frequency of the extracted component, i.e. sun gear or planet gear. In this case one has to take into account the Willis formula. If f_p is the rotation frequency of the planet gear and f_c is the rotation frequency of the planet carrier, then the relation between cyclic frequency and cyclic order for the planet gear is $|f_p - f_c| = 11.0769\text{Hz}$.

Figure 18 shows the Cyclic Power evaluated on the extracted planet signals in both sound and faulty conditions in the cyclic order range $0 \div 12$. In the Cyclic Power of the sound planet (Figure 18(a)), three distinct components are visible. The first one (0.36O) is related to the rotation of the first stage planet carrier, whilst the others (2O and 6O) are linked to the planet rotation frequency. On the contrary, Figure 18(b) shows the presence of two distinct cyclic orders, the first one (2O) is related to the planet rotation frequency, while the second one (9.6O) is the inner race fault order of the planet bearing. By comparing Figures 17 (b) and 18(b) it is possible to see that, in order to diagnose a fault inside a planet bearing, the planet signal must be extracted from the main vibration signal. Sure enough, the cyclic fault frequency is not visible in the Cyclic Spectrum of the main vibration signal (Figure 17 (b)), but only in the Cyclic Spectrum of the planet gear signal (Figure 18(b)).

It must be pointed out the importance of the pre-processing performed on the basis of tooth mesh period in the bearing analysis. Usually the bearing fault frequencies and the gear frequencies cover different ranges of the spectrum, how can the proposed method be able to retrieve bearing information under these circumstances? It is a matter of fact that the cause of the vibration signal, i.e. the fault on the bearing, is strictly related to two elements: the geometry of system, and the kinematics of the system. It is well known there is a direct proportionality between the fault frequency, the geometry of the bearing and the rotational frequency of moving ring (kinematics). In common applications both the geometry and kinematics are given, as in an asynchronous motor working at constant speed. In other applications like the planetary gearbox, the bearing could be placed on subsystems (i.e. the carrier) whose kinematics depends on other mechanisms kinematics (the sun and the ring gears). Moreover, the relative position between the source of the vibration (i.e. the bearing) and the sink (i.e. the sensor) changes cyclically. A simple, although direct, analysis of the raw data will comprise these non-trivial aspects. The extraction of the signal of the signal on the basis of the tooth mesh period allows rebuilding a new vibration data on the basis of both geometry and kinematics of the gearbox. Please note the fundamental difference between the gear and bearing diagnostics: both start from the reconstruction of the vibration signal of the planet, but the gear analysis needs a further processing by means of TSA, while the bearing analysis is performed on the reconstructed signal directly.

5. Concluding Remarks

In this paper a comprehensive diagnostics of the two main components of a gearbox is presented. In the available literature papers focus on gears and bearings separately, leaving a sensible gap anytime the whole gearbox needs to be monitored. In particular, this paper addresses the diagnostics of epicyclic gearboxes, which are more complex than ordinary ones. In fact the relative angular position among an external accelerometer, the planet and sun gears is cyclic, and a vibration signal of a faulted tooth planet could be dominated by the vibration of another planet closer to the sensor. Two procedures for the precise evaluation of the planet gear position have been presented. The first one is based on the study of the power flows inside the ring gear TSA, whilst the second method is based on a modified statistical parameter such as the Crest Factor (MCF). The effectiveness of the two methods are compared on the basis of real data.

In the first method the position of the planet gears with respect to the transducer is obtained by reconstructing the power flow at the cyclic frequency corresponding to the number of planet gears of the planetary gearbox under test. The second method relies on a modified version of the Crest

Factor (MCF). In particular, the MCF is evaluated on a tooth-wide signal portion, thus obtaining a function and not a single value. The planet gear position is determined by filtering the so obtained MCF around the frequency related to the number of planet gears.

The two proposed methods give the same results, highlighting the position of the planet gears. As these positions are completely determined by the maxima of the two functions, the entire procedure could be easily automated.

From the present analysis it could be concluded that the evaluation of the relative position between planet gears and transducer is a useful information for the effectiveness of the averaging procedure, in particular for flat shaped transfer function of the gearbox. Actually, if the correct position of the planet gear with respect to the transducer is not correctly determined, the signature of the faulty planet gear cannot be extracted from noisy vibration responses.

The same procedure allows to deduce further informations on planet bearings health condition. Planet bearings are full-complement needle bearings without cage. This arrangement consists of a collection of rollers arranged loosely between the pin, which connects the gear to the carrier, and the bore of the gear. A localised fault was artificially introduced on the inner ring of a planet bearing (carrier's pin) via a drilling process in order to prove the effectiveness of the procedure.

In particular the evaluation of the Cyclic Power on the rebuilt signal allows to obtain information on how the power is released. The results indicate that the proposed methodology can identify the faulted bearing signature.

6. Acknowledgement

This work has been developed within the Advanced Mechanics Laboratory (MechLav) of Ferrara Technopole, realized through the contribution of Regione Emilia-Romagna - Assessorato Attivitá Produttive, Sviluppo Economico, Piano telematico - POR-FESR 2007-2013, Attivitá I.1.1

7. References

[1] Antoni, J., Bonnardot, F., Raad, A., El Badaoui, M.: Cyclostationary modelling of rotating machine vibration signals. Mechanical Systems and Signal Processing 18, 1285-1314 (2004)

[2] Gardner, W.A.: The spectral correlation theory of cyclostationary time-series. Signal Processing 11(1), 13-36 (1986)

[3] McCormick, A.C., Nandi, A.K.: Cyclostationary in rotating machine vibrations. Mechanical Systems and Signal Processing 12, 225-242 (1998)

[4] Randall, R.B., Antoni, J.: Rolling element bearing diagnosticsA tutorial. Mechanical Systems and Signal Processing 25, 485-520 (2011)

[5] Antoni, J.: Cyclic spectral analysis of rolling-element bearing signals: Facts and fictions. Journal of Sound and Vibration 304, 497-529 (2007)

[6] Antoni, J.: Cyclostationarity by examples. Mechanical Systems and Signal Processing 23, 987-1036 (2009)

[7] S. Braun, *The extraction of periodic waveform by time domain averaging*, Acustica, Vol. 32, No. 2, 1975, pp. 69-77.

[8] P. D. McFadden, *Interpolation techniques for time domain averaging of gear vibration*, Mechanical Systems and Signal Processing, Vol. 3, No. 1, January 1989, pp. 87-97.

[9] S. Braun, *The synchronous (time domain) average revisited*, Mechanical Systems and Signal Processing, Vol. 25, No. 4, May 2011, pp. 1087-1102.

[10] P. D. McFadden, *A technique for calculating the time domain averages of the vibration of the individual planet gears and sun gear in an epicyclic gearbox*, Journal of Sound and Vibration, Vol. 144, No. 1, 1991, pp. 163-172.

[11] D. Forrester, *A method for the separation of epicyclic planet gear vibration signatures*, Acoustical and Vibratory Surveillance Methods and Diagnostic Techniques, Senlis, France, October 1998

[12] P.D. Samuel and D.J. Pines, *Vibration separation and diagnostics of planetary geartrains*, American Helicopter Society 56th Annual Forum, Virgian Bearch, Va, May 2000.

[13] P.D. McFadden, *Window Functions for the Calculation of the Time Domain Averages of the Vibration of the Individual Planet Gears and Sun Gear in an Epicyclic Gearbox*, Journal of Vibration and Acoustics, Vol. 116, 1994, pp. 179-187.

[14] P.D. McFadden and J.D. Smith, *An explanation for the asymmetry of the modulation sidebands about the tooth meshing frequency in epicyclic gear vibration*, Journal of Mechanical Engineering Science, Vol. 199, No. C1, 1985, pp. 65-70.

[15] P. D. McFadden, *Detecting Fatigue Cracks in Gears by Amplitude and Phase Demodulation of the Meshing Vibration*, Journal of Vibration, Acoustics, Stress and Reliability in Design, Vol. 108, 1986, pp. 165-170

[16] J.I. Taylor, *The Gear Analysis Handbook*, Tampa (FL), USA, Vibration Consultants Inc., 2000.

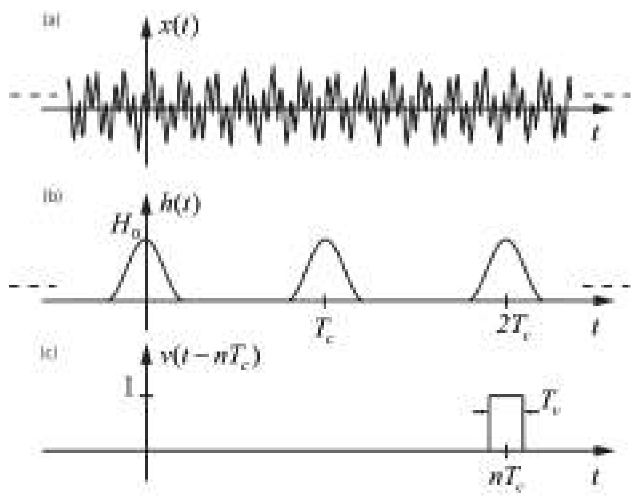

Figure 1: Planet vibration signal measured by a fixed transducer [10]: (a) Time planet vibration signal, (b) Transfer function between planet and transducer (c) windowing function $v(t - nT_c)$, where n is an integer number

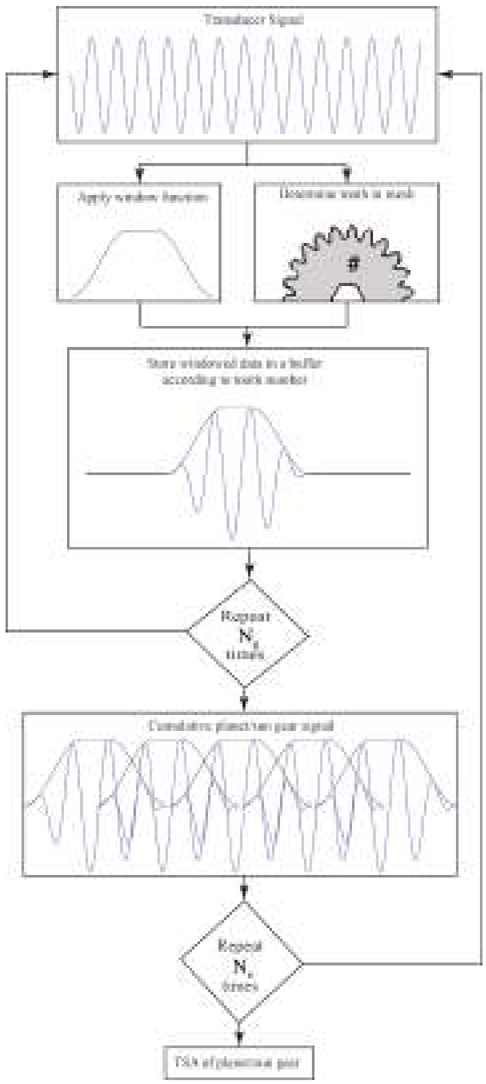

Figure 2: TSA block diagram for planet/sun gear. N_g is the tooth number of the gear of interest. N_e is the number of averages.

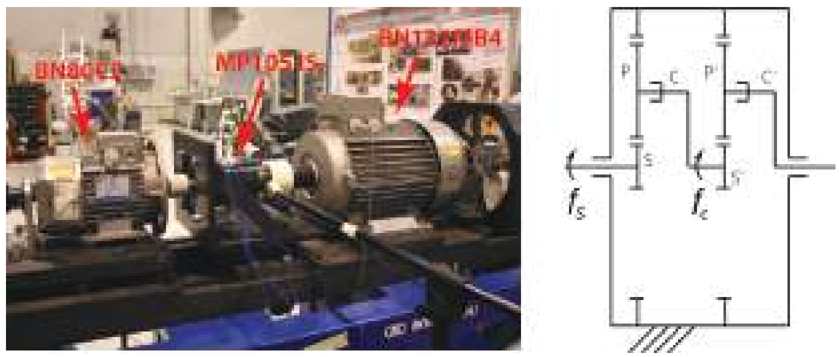

Figure 3: Test-rig

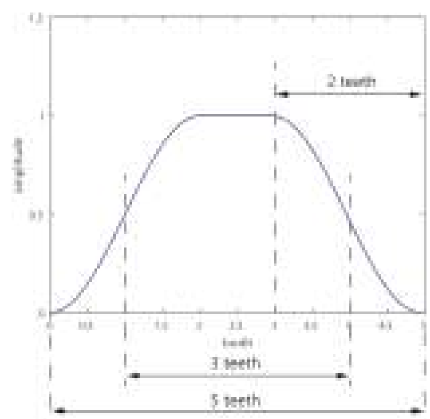

Figure 4: Window function used in the TSA algorithm

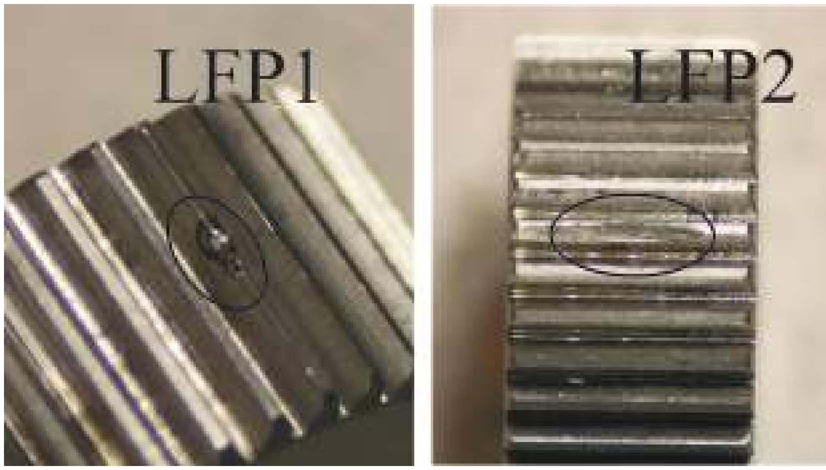

Figure 5: Localised tooth faults

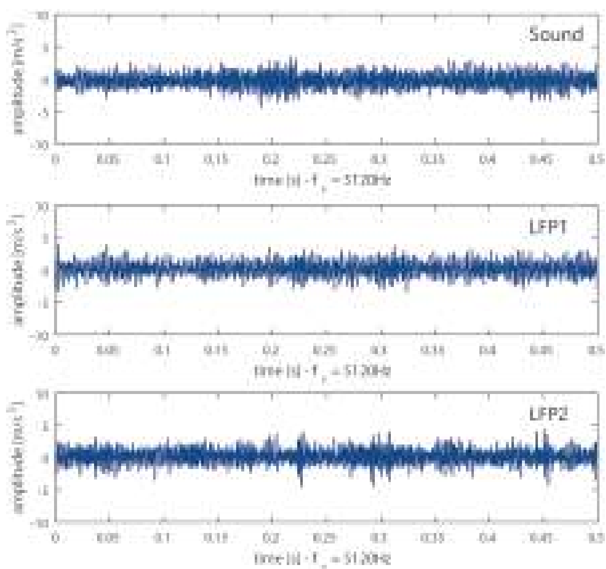

Figure 6: Time signal for two revolutions of the planet carrier: Sound, LFP1 fault, LFP2 fault

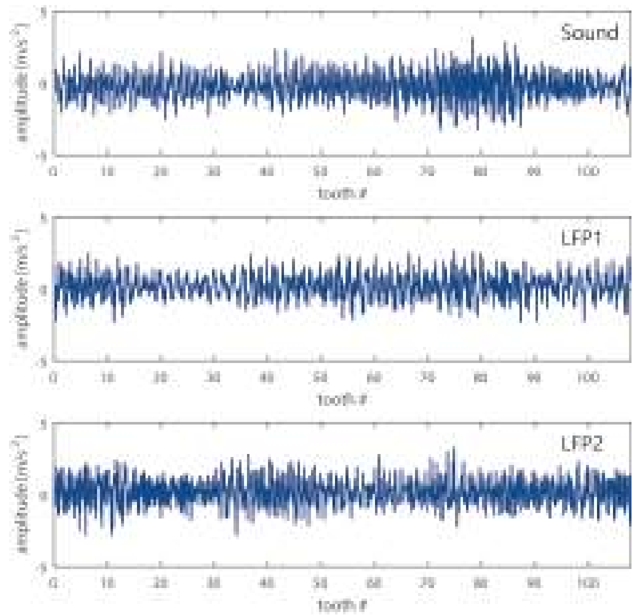

Figure 7: Ring gear TSA (246 averages): Sound, LFP1 fault, LFP2 fault

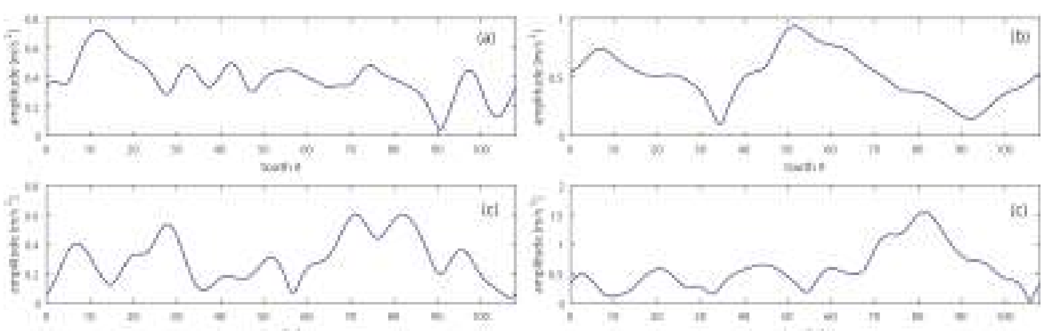

Figure 8: Amplitude modulation of sound ring gear TSA: (a) filtered around the first meshing component, (b) filtered around the second meshing component, (c) filtered around the third meshing component, (d) filtered around the fourth meshing component

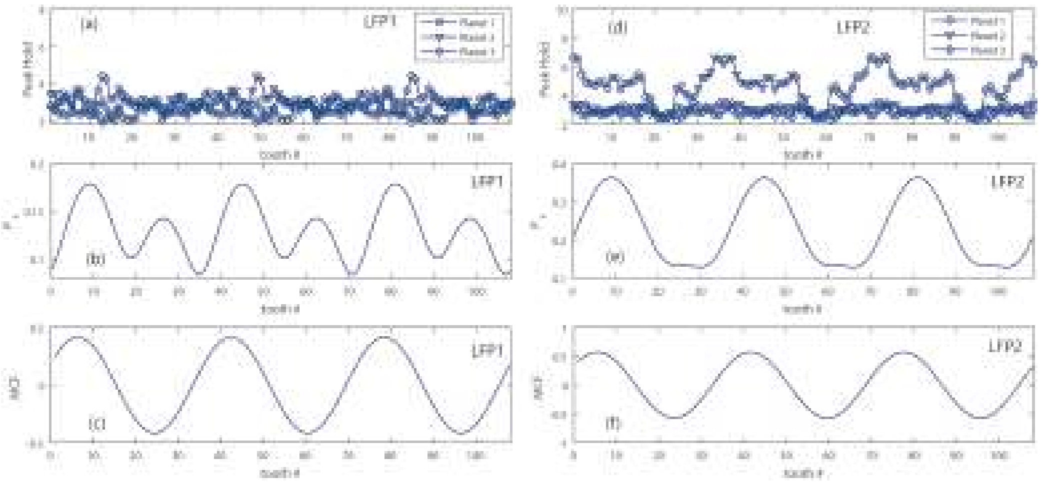

Figure 9: (a) Peak Hold of the planet gear vibrations extracted with an increasing shift from 1 to 108 ring gear tooth for the LFP1 fault, (b) P_x function for the LFP1 fault, (c) MCF function for the LFP1 fault, (d) Peak Hold of the planet gear vibrations extracted with an increasing shift from 1 to 108 ring gear tooth for the LFP2 fault, (e) P_x function for the LFP2 fault, (e) MCF function for the LFP2 fault

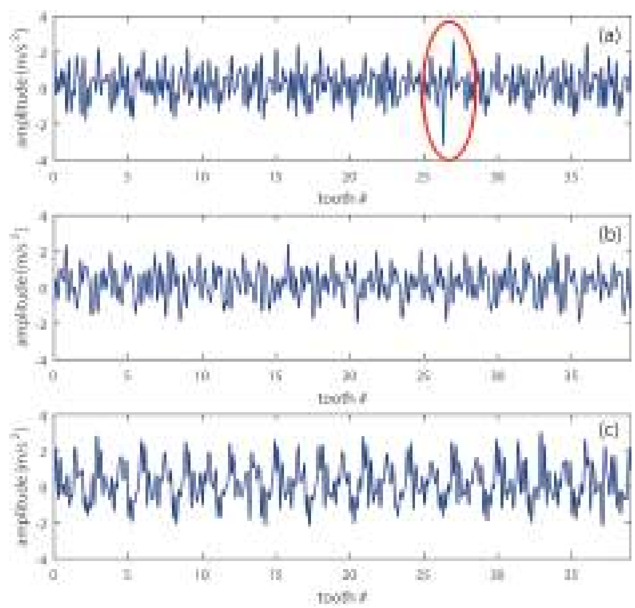

Figure 10: TSA of planet gears for LFP1 fault with an initial phase shift of 8 teeth (18 averages): (a) Planet gear 1, (b) Planet gear 2, (c) Planet gear 3

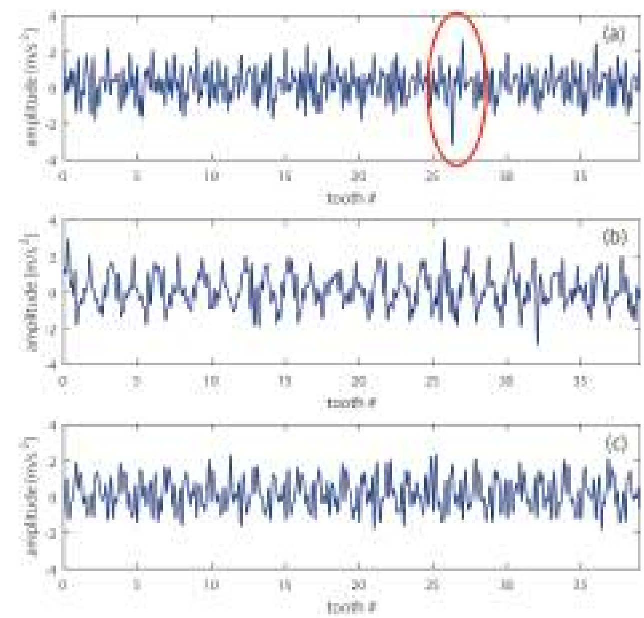

Figure 11: TSA of planet gear 1 for LFP1 fault (18 averages): (a) initial phase shift of 8 teeth, (b) initial phase shift of 35 teeth, (c) initial phase shift of 62 teeth

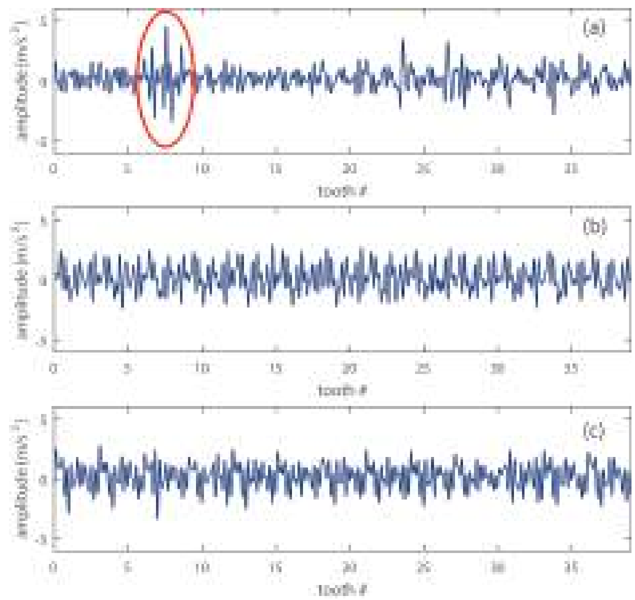

Figure 12: TSA of planet gears for LFP2 fault with an initial phase shift of 8 teeth (18 averages): (a) Planet gear 1, (b) Planet gear 2, (c) Planet gear 3

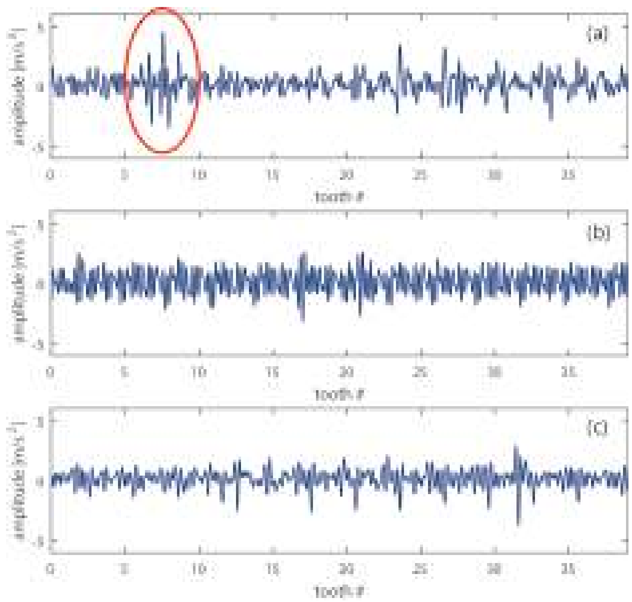

Figure 13: TSA of planet gear 1 for LFP2 fault (18 averages): (a) initial phase shift of 8 teeth, (b) initial phase shift of 35 teeth, (c) initial phase shift of 62 teeth

Figure 14: (a) planet gear full-complement needle bearing, (b) localised fault on the inner race (cage pin) of a planet bearing

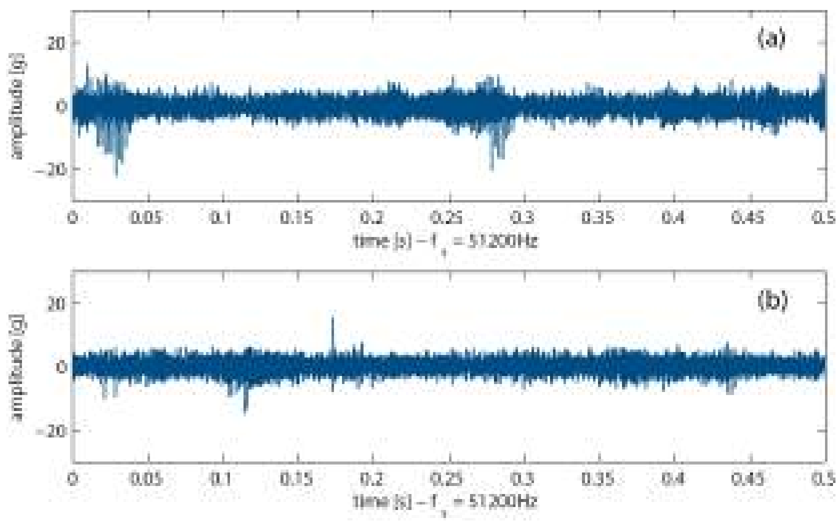

Figure 15: Time signal for 2 revolutions of the planet carrier: (a) Sound, (b) Faulty

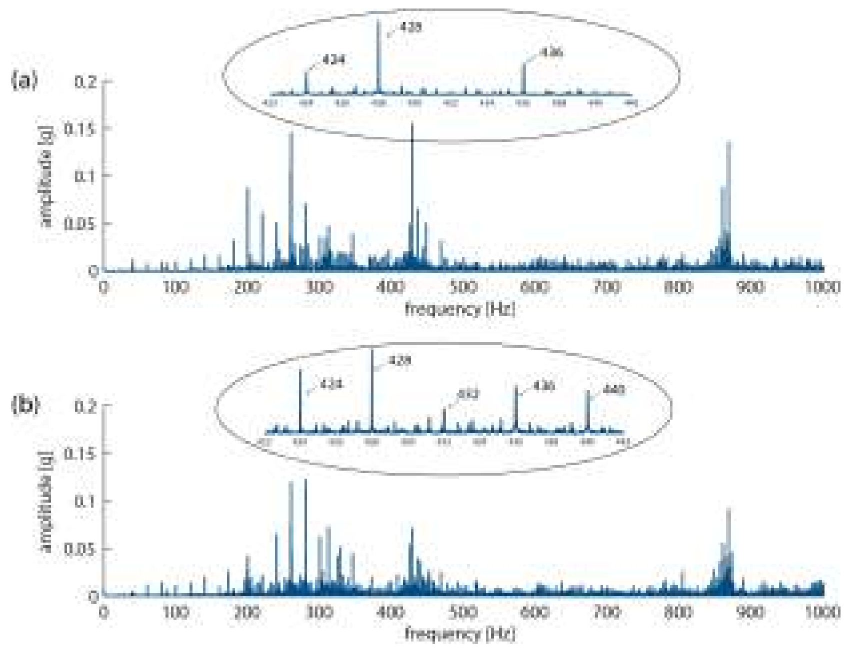

Figure 16: Spectra: (a) Sound, (b) Faulty

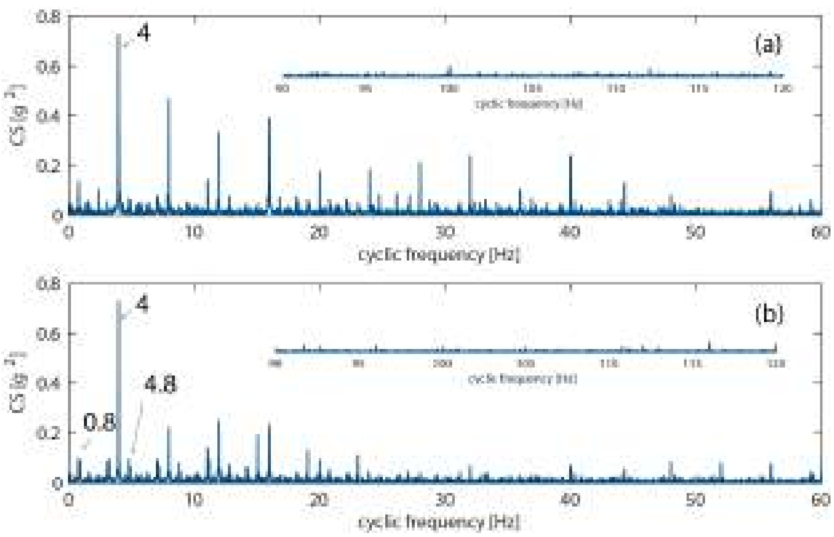

Figure 17: Cyclic Power evaluated on the time signal: (a) Sound, (b) Faulty

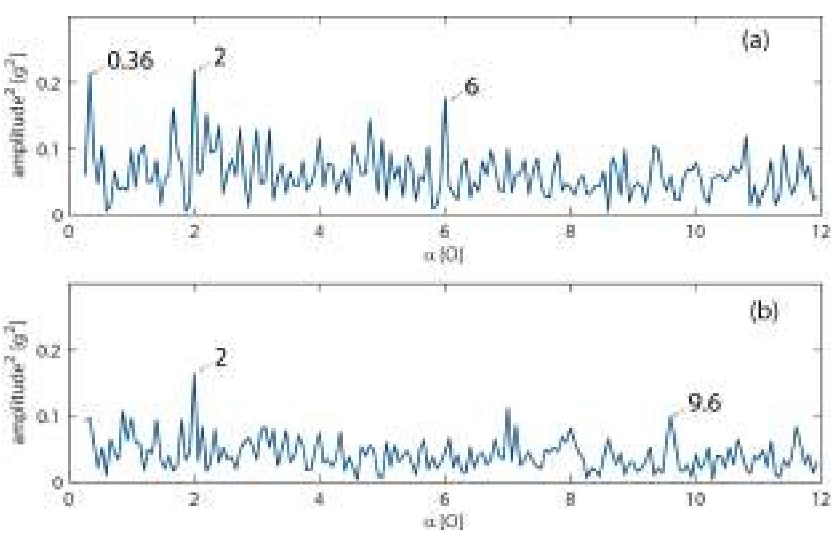

Figure 18: Cyclic Power evaluated on the extracted planet signal: (a) Sound, (b) Faulty